Cloud Optical Properties from the Multi-Filter Shadowband Radiometer (MFRSRCLDOD): An ARM Value-Added Product

December 2004

David D. Turner
Chaomei Lo
Pacific Northwest National Laboratory – Richland, Washington

Qilong Min
State University of New York (SUNY) – Albany, New York

Contents

Figures

Tables

1. Introduction

The microphysical properties of clouds play an important role in studies of global climate change. Observations from satellites and surface-based systems have been used to infer cloud optical depth and effective radius. Min and Harrison (1996) developed an inversion method to infer the optical depth of liquid water clouds from narrow band spectral multi-filter rotating shadowband radiometer (MFRSR) measurements (Harrison et al. 1994). Their retrieval also uses the total liquid water path (LWP) measured by a microwave radiometer (MWR) to obtain the effective radius of the warm cloud droplets. Their results were compared with Geostationary Operational Environmental Satellite (GOES) retrieved values at the Atmospheric Radiation Measurement (ARM) Southern Great Plains (SGP) site (Min and Harrison 1996). Min et al. (2003) also validated the retrieved cloud optical properties against in situ observations, showing that the retrieved cloud effective radius agreed well with the in situ forward scattering spectrometer probe (FSSP) observations. The retrieved cloud optical properties from Min et al. (2003) were used also as inputs to an atmospheric shortwave model, and the computed fluxes were compared with surface pyranometer observations.

The Min and Harrison algorithm has been incorporated into an ARM Value-Added Product (VAP) called MFRSR CLDOD. This version of the VAP (1Min) uses the diffuse transmission at 415 nm from the MFRSR. Therefore, the results are only valid for "horizontally homogeneous" stratiform clouds with optical depths larger than approximately 7. The retrieval assumes a single cloud layer consisting solely of liquid water drops. As specified by Min and Harrison (1996), the wavelength at 415 nm was chosen due to the lack of gaseous absorption and the relatively constant surface albedo (in the absence of snow) at this wavelength.

The MFRSR CLDOD VAP (henceforth referred to as "the VAP") retrieves cloud optical depth (τ) from the MFRSR measurements. If the LWP is available from a coincident MWR observation, then the droplet effective radius (r_e) can be determined. Knowledge of the estimated r_e can be used to improve the estimate of τ because there is a slight dependence on the extinction coefficient, single scattering albedo, and asymmetry parameter on effective radius at this wavelength. However, if the MWR's LWP is not available, then the VAP assumes that $r_e = 8.0$ μm. The primary output from the VAP is τ and r_e.

The VAP also provides 1-sigma uncertainties for τ and r_e by propagating the uncertainties in the top-of-atmosphere irradiance (I_0), the measured irradiance (I), the MWR's LWP, and the surface albedo.

2. Input Data

The input files for this VAP are standard ARM NetCDF products. To run this VAP properly, we need the following input files and data for the SGP site:[1]

Multi-Filter Rotating Shadowband Radiometer instrument:

sgpmfrsrE13.b1 – 20 s data

This data stream contains the observed irradiance data (I) from the MFRSR.

---

[1] For details of the input variables, see Appendix A.

Microwave Radiometer instruments:

sgpmwrlosC1.a1

    The LWP from the MWR.

Langley Value Added Project:

sgpmfrsrLangleyE13.c1 – 2 data points per day

    This VAP provides the top of atmosphere irradiance (I_0) data.

Short Wave Flux Value Added Project:

sgp15swfanalsirs1longC1.c1

    This VAP provides ancillary data for future analyses regarding the cloud sky cover fraction.

Cloud Base Height Value Added Project:

sgparsclbnd1clothC1.c1

    This VAP provides ancillary data for future analyses regarding the height (and by inference the phase) of the clouds.

3. Output Data

The name of the output file is:

    sgpMFRSRCldOD1MinE13.C1.YYYYMMDD.hhmmss – 20 s data

    Where:
SGP	–	the site of the instrument
MFRSR	–	the main instrument name
CldOD1Min	–	identifies that this is Min's version 1 VAP
E13	–	facility
YYYY	–	year, MM - month of the year, DD - day of the month, hh - hour of the day, mm - minute of the hour, ss - second of the minute of data start

    The detailed variable description is in Table 2 of Appendix B.

This VAP generates two quicklook plots: one is the I_0 calibration in Figure 1 and the second is the cloud optical properties in Figure 4. The names of the quicklook files are

YYYYMMDD_quicklook.png

Io_YYYYMMDD_quicklook.png

4. Algorithm/Method

The functioning heart of this VAP is the Nonlinear Least Squares retrieval algorithm of Min and Harrison (1996). This algorithm uses a parameterization of the scattering properties at 415 nm on the effective radius and LWP using Mie theory. The algorithm uses an adjoint formulation of the radiative transfer to maintain accuracy and improve its execution speed. It uses an iterative approach to retrieve both cloud optical depth and effective radius if an estimate of LWP is provided; otherwise the effective radius is assumed and the algorithm returns only optical depth.

The algorithm requires the atmospheric transmittance at 415 nm. This is easily computed using the observed irradiance I and the top of the atmosphere irradiance I_0, where I_0 is computed from Langley regressions on clear days. Because data from the MFRSR are used to obtain both I and I_0, the absolute calibration of the instrument is not required to get accurate observations of the atmospheric transmittance.

A previously developed VAP routinely analyzed the MFRSR data and computes I_0. However, the most accurate values of I_0 are obtained only on days that are free of clouds and stable. Furthermore, a maximum of two Langley regressions could be computed for a single day. Because this VAP is concerned with cloud properties, the I_0 values used are computed from I_0 values determined on nearby clear sky days. We have automated a procedure to determine an accurate value of I_0. The VAP reads in all of the I_0 data that were determined to be good by the Langley analysis VAP for 3 months before and after the day currently being processed. From this large dataset, we select the 20 closest in time I_0 values. We then follow the procedure outlined in Michalsky et al. (2001) to select the best 10 of the 20 points; the mean value of these 10 points is used as the I_0 for the processing. The uncertainty in I_0 represented by the standard deviation about the mean I_0 value of the 10 points is propagated to provide uncertainties in the retrieved cloud properties. Figure 1 shows a quicklook plot that displays all of the I_0 values determined by the Langley algorithm VAP, the 20 closest points, and the mean and standard deviation of the I_0 value used in the VAP.
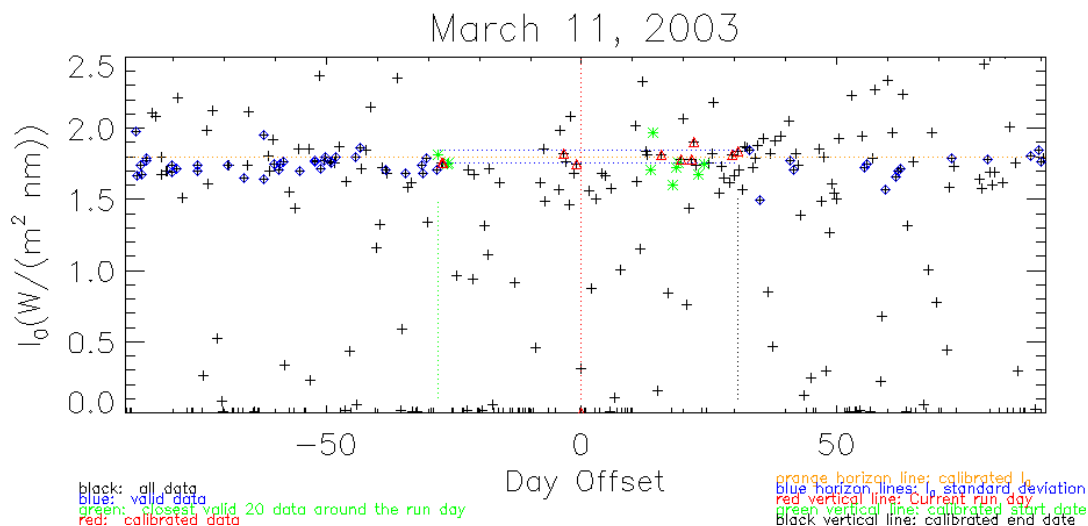
Figure 1. I_0 Calibration quicklook plot. See text for details.

The LWP from the MWR, while not critical for the execution of the VAP, does permit the retrieval of effective radius. The VAP applies some simple quality control to ensure that the reported LWP is valid. If the observed brightness temperature at either MWR frequency is below the cosmic background or above 100K (the latter condition is usually indicative of rain) then the LWP value from the MWR is not used in the retrieval. Furthermore, because the uncertainty in the MWR's retrieval LWP is approximately 20 g m^{-2} (Westwater et al. 2001), the VAP does not use the MWR's observed LWP in the retrieval if the LWP is below this threshold. When no LWP is available, the retrieval algorithm assumes that the effective radius is 8 μm.

The temporal resolution of the MFRSR irradiance data is 20 s, and therefore the ancillary inputs are interpolated to this time. The interpolation of the LWP is usually required. The LWP is interpolated across gaps of a maximum of 5 min. If the temporal gap is larger than this, then the retrieval is run without LWP input for those MFRSR samples.

Because this VAP can be run at sites that has a MFRSR, such as the ARM extended facilities, the VAP uses the retrieved optical depth and assumed effective radius to provide an estimate of the LWP using

$$LWP = (2/3) * \rho * \tau * r_e$$

Where ρ is the density of liquid water, τ is retrieved by the VAP, and r_e was assumed. This provides estimates of the LWP at sites where MWRs are not deployed. However, due to the natural variability in r_e the uncertainty in this derived LWP is large. A flag is set in the output file to indicate if the output LWP is from the MWR or this calculation.

4

The retrieval algorithm operates at two temporal resolutions. It provides "instantaneous" retrievals at the nominal 20 s resolution of the MFRSR and "average" retrievals where the data have been averaged for 5 min centered upon the ouput sample time. The average retrievals are less sensitive to the spatial inhomogenialties in the cloud, which affect the diffuse irradiance field.

As indicated above, the VAP provides 1-sigma uncertainties for both the retrieved optical depth and effective radius by propagating the uncertainties in the input and assumed parameters. The uncertainty in the I_0 value is the standard deviation about the mean I_0 as described above. If the LWP is available from the MWR, the uncertainty in the LWP is assumed to be 20 g m^{-2}. The uncertainty in the observed irradiance is assumed to be 1%. The surface albedo, which is taken to be 0.036 at 415 nm in non-snow covered conditions, is assumed to have an uncertainty of ±0.01. These uncertainties are propagated individually using finite differences and combined as the root sum of squared errors (i.e., these uncertainties are assumed to be independent). The uncertainty in the retrieved optical depth is dominated by the uncertainty in I_0, while the uncertainty in the LWP is the dominant term in the effective radius uncertainty. Figures 2 and 3 present examples of distributions of each component of the total uncertainty to the uncertainty in τ and r_e, respectively, as well as the distributions of the total uncertainty in each retrieved variable for data from the SGP site over a 6-month period.

Finally, this VAP provides some ancillary data to help the analyst find cases where the retrieval is valid. The fractional sky cover from the shortwave analysis VAP (Long and Gaustad 2004) is included because the retrievals from this VAP are only valid in overcast scenes. The cloud base height from the active remote sensing clouds (ARSCL) VAP (Clothiaux et al. 2001), along with the infrared thermometer (IRT) sky brightness temperature, are included because the retrievals are also only valid for single layer liquid water clouds. Therefore, the user should use these fields to help select the proper cases to analyze.
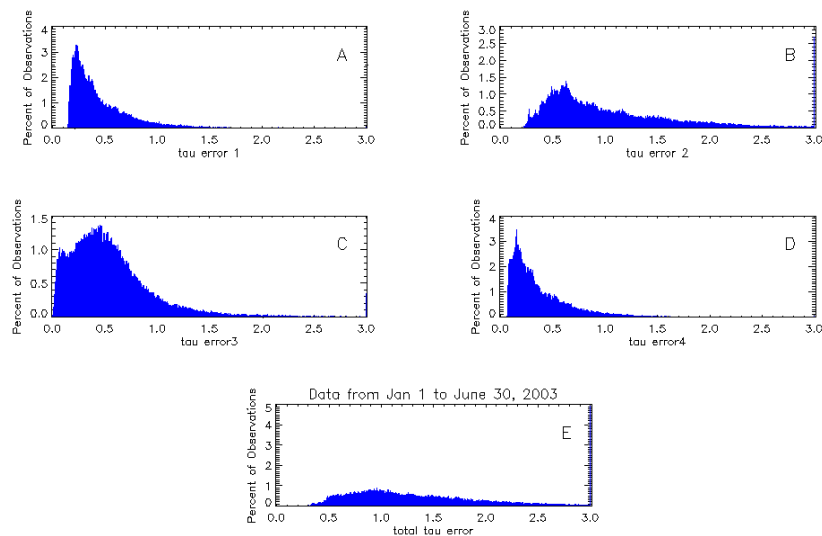
Figure 2.   Distribution of the uncertainties in cloud optical depth for uncertainties in A) I, B) I_0, C) LWP, D) surface albedo. Panel E shows the distribution of the total uncertainty in the cloud optical depth for this 6-month period (Jan – Jun 2003)
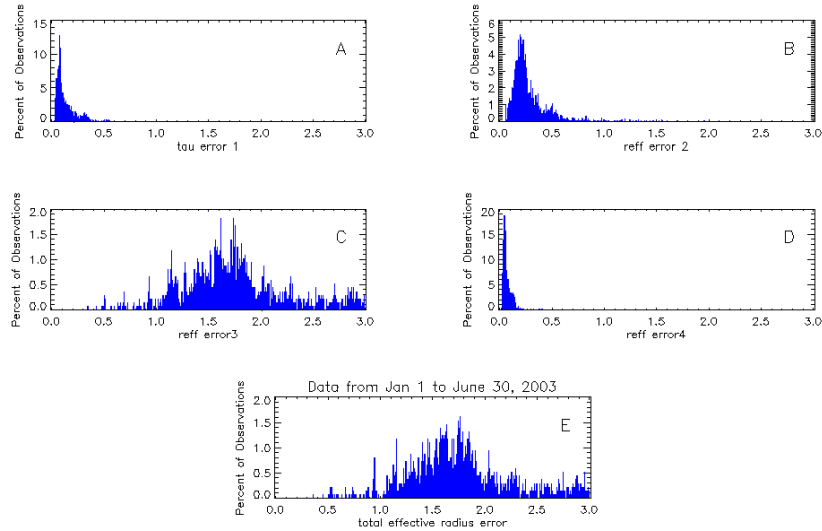
Figure 3. Distribution of the uncertainties in effective radius for uncertainties in I, B) I_0, C) LWP, D) surface albedo. Panel E shows the distribution of the total uncertainty in the cloud optical depth for this 6-month period (Jan – Jun 2003)

5. Examples

This VAP runs on the daily basis. There are two quicklook plots generated everyday, one is the I_0 calibration in Figure 1 as explained before and the other one is a five-panel plot for the cloud properties. Figure 4 gives an example for March 11, 2003. The data start around 13:50 Universal Time Coordinates (UTC) and ends around 24:00. An overcast liquid water cloud persisted on this day, as the clouds were of low height and the effective radius was small indicating the presence small cloud drops. The first panel shows the derived cloud optical depth data for instantaneous (20 s) and averaged (5-min) resolutions. The second panel shows the retrieved effective radius. The third panel shows the ratios of the total uncertainty to the retrieved data. Panel four displays the cloud fraction and cloud height. The last panel shows the LWP from MWR or the LWP from the default effective radius (which it does not have on this day, because all of the MWR LWP data were valid).

The six months of data from January 1 to June 30, 2003, are show in Figure 5 and the distributions of the cloud properties for this period are shown in Figure 6. Only valid data meeting the following criterion are included in Figures 5 and 6. The criteria are cloud fraction > 90 %, infrared temperature > 268 (-50°C), cloud base height < 4 km, optical depth > 7, effective radius $\neq$ 8.00 μm (because an effective radius equal to 8 μm implies that the LWP from the MWR was not available or not used), and effective radius > 0.
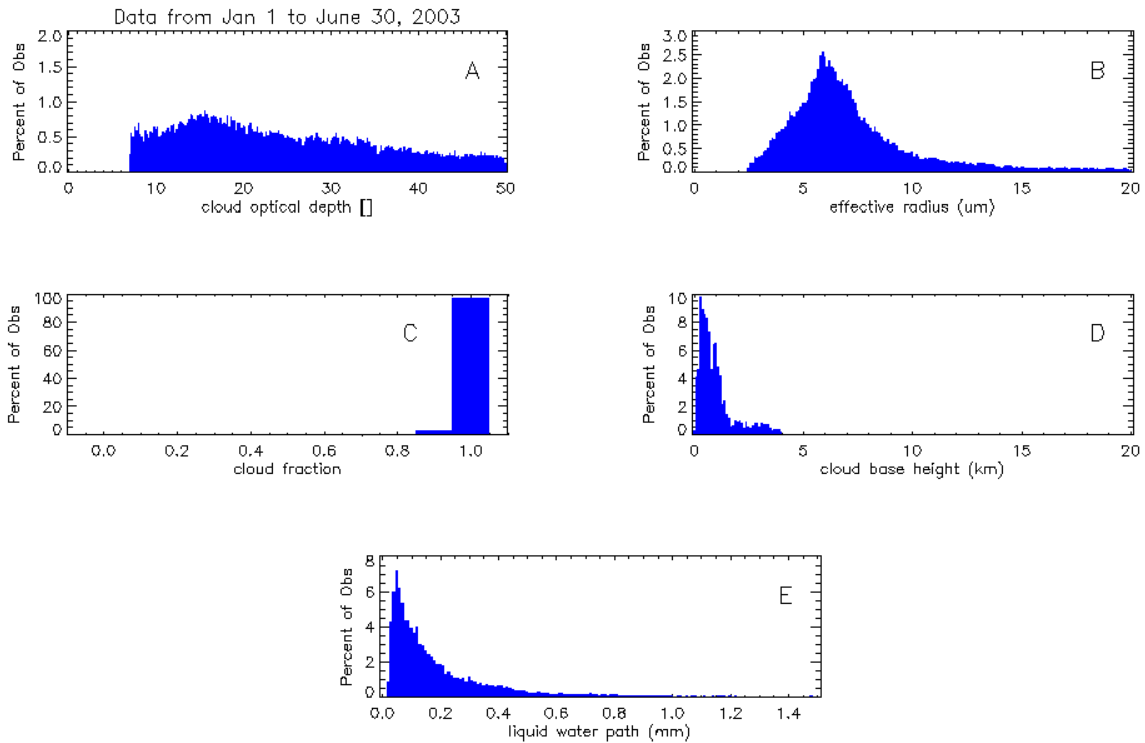
6
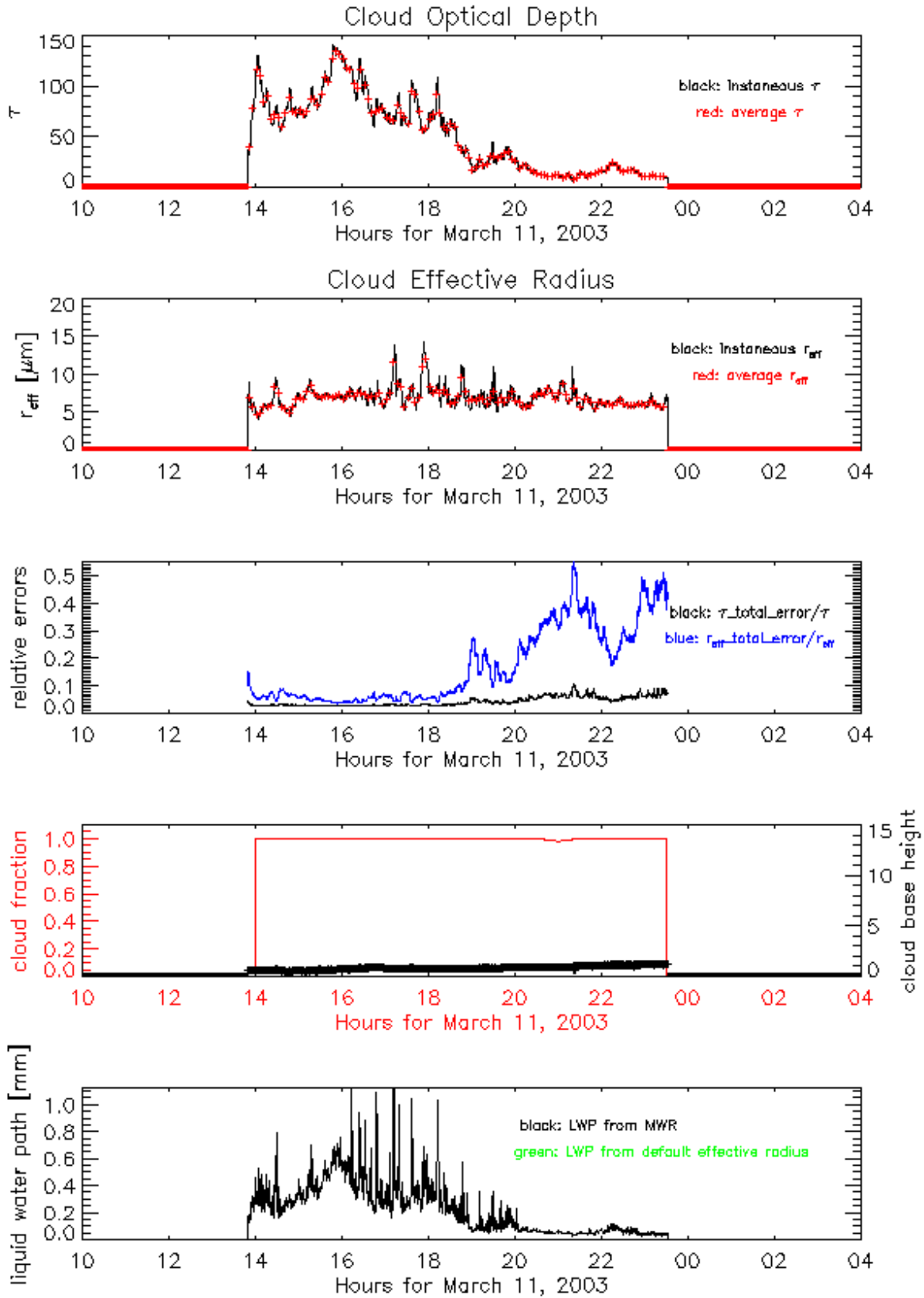
Figure 4.   Quicklook image showing the cloud optical properties for March 11, 2003
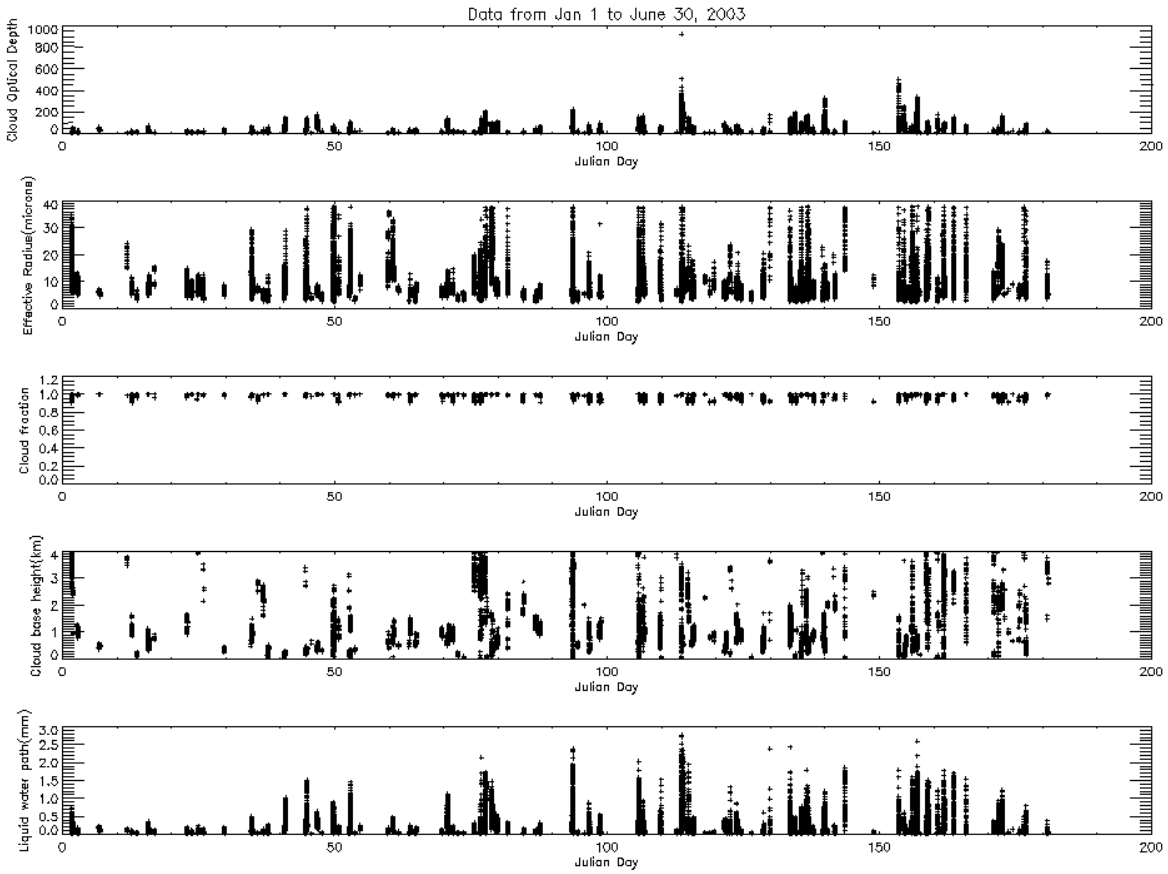
Figure 5. Retrieved cloud optical properties for 6 months of data starting 1 Jan 2003. A) retrieved τ, B) retrieved r_e, C) cloud fraction from shortwave flux analysis VAP, D) cloud base height from ARSCL VAP, E) LWP from the MWR.

Figure 6. Distributions of the retrieved cloud optical depth (A) and effective radius (B) from 1 Jan to 30 June 2003. Panel C, D and E show the corresponding cloud fraction, cloud height and LWP

6. Known Caveats

- Only valid for overcast conditions where cloud is liquid. Because there is no gaseous absorption at this wavelength (415 nm), the retrieval will be valid for both single layer and multiple layer cloud conditions, as long as all layers are overcast and composed entirely of liquid drops.

- Assumes the surface is not covered with snow or ice.

- Biases in the MWR's LWP, especially for small optical depths, will bias the retrieved effective radius.

7. References

Clothiaux, EE., MA Miller, RC Perez, DD Turner, KP Moran, BE Martner, TP Ackerman, GG Mace, RT Marchand, KB Widener, DJ Rodriguez, T Uttal, JH Mather, CJ Flynn, KL Gaustad, and B Ermold. 2001. The ARM millimeter wave cloud radars (MMCRs) and the active remote sensing of clouds (ARSCL) Value Added Product (VAP). ARM-TR-002-1. U.S. Department of Energy. Available at http://www.arm.gov/publications/tech_reports/armvap-002-1.pdf.

Harrison, LC, JJ Michalsky, and J Berndt. 1994. "Automated multi-filter rotating shadowband radiometer: an instrument for optical depth and radiation measurements." *Applied Optics* 33:5126-5132.

9

Long, CN, and KLGaustad. 2004. The shortwave (SW) clear-sky detection and fitting algorithm: algorithm operational details and explanations. Revision 1. ARM-TR-004-1. U.S. Department of Energy. Available at http://www.arm.gov/publications/tech_reports/arm-tr-004-1.pdf.

Michalsky, JJ, JA Schlemmer, WE Berkheiser, JL Berndt, LC Harrison, NS Laulainen, NR Larson, and JC Barnard. 2001. "Multiyear measurements of aerosol optical depth in the Atmospheric Radiation Measurement and Quantitative Links programs." *Journal of Geophysical Research* 106:12099-12107.

Min, Q and LC Harrison. 1996. "Cloud properties derived from surface MFRSR measurements and comparison with GOES results at the ARM SGP site." *Geophysical Research Letters* 23:1641-1644.

Min, Q, M Duan, and R Marchand. 2003. "Validation of surface retrieved cloud optical properties with in situ measurements at the Atmospheric Radiation Measurement Program (ARM) South Great Plains site." *Journal of Geophysical Research* 108, 4547, doi:10.1029/2003JD003385.

Westwater,E.R., Y Han, MD Shupe, SY Matrosov. 2001. "Analysis of integrated cloud liquid and precipitable water vapor retrievals from MWRs during SHEBA." *Journal of Geophysical.Res*earch 106: 32,019-32,030.

Appendix A - Input Data

Table 1 lists the various ARM data streams used in the VAP for data, along with the specific variables in files that are used in processing.

Table 1.   Input Variables

Data Stream	Variable Name	Variable Long Name	Units
sgpmfrsrE13.b1	cosine_solar_zenith_angle	Cosine Solar Zenith Angle	unitless
	hemisp_narrowband_filter1	Narrowband Hemispheric Irradiance, Filter 1	$W/(m^2\,nm)$
	hemisp_narrowband_filter2	Narrowband Hemispheric Irradiance, Filter 2	$W/(m^2\,nm)$
	hemisp_narrowband_filter3	Narrowband Hemispheric Irradiance, Filter 3	$W/(m^2\,nm)$
	hemisp_narrowband_filter4	Narrowband Hemispheric Irradiance, Filter 4	$W/(m^2\,nm)$
	hemisp_narrowband_filter5	Narrowband Hemispheric Irradiance, Filter 5	$W/(m^2\,nm)$
	direct_normal_narrowband_filter1	Narrowband Direct Normal Irradiance, Filter 1	$W/(m^2\,nm)$
	direct_normal_narrowband_filter2	Narrowband Direct Normal Irradiance, Filter 2	$W/(m^2\,nm)$
	direct_normal_narrowband_filter3	Narrowband Direct Normal Irradiance, Filter 3	$W/(m^2\,nm)$
	direct_normal_narrowband_filter4	Narrowband Direct Normal Irradiance, Filter 4	$W/(m^2\,nm)$
	direct_normal_narrowband_filter5	Narrowband Direct Normal Irradiance, Filter 5	$W/(m^2\,nm)$
sgpmwrlosC1.b1	vap	Total water vapor along LOS path	cm
	liq	Total liquid water along LOS path	cm
	tbsky23	23.8 GHz sky brightness temperature	K
	tbsky31	31.4 GHz sky brightness temperature	K
	sky_ir_temp	IR Brightness Temperature	K
sgpmfrsrlangleyE13.c1	barnard_solar_constant_sdist_filter1	solar constant corrected for solar distance for the Direct Narrowb and Filter 1	$W/(m^2\,nm)$
	barnard_solar_constant_sdist_filter2	solar constant corrected for solar distance for the Direct Narrowb and Filter 2	$W/(m^2\,nm)$
	barnard_solar_constant_sdist_filter3	solar constant corrected for solar distance for the Direct Narrowb and Filter 3	$W/(m^2\,nm)$
	barnard_solar_constant_sdist_filter4	solar constant corrected for solar distance for the Direct Narrowb and Filter 4	$W/(m^2\,nm)$
	barnard_solar_constant_sdist_filter5	solar constant corrected for solar distance for the Direct Narrowb and Filter 5	$W/(m^2\,nm)$
	barnard_badflag_filter1	rejection flag for Direct Narrowband Filter 1	unitless
	barnard_badflag_filter2	rejection flag for Direct Narrowband Filter 2	unitless
	barnard_badflag_filter3	rejection flag for Direct Narrowband Filter 3	unitless
	barnard_badflag_filter4	rejection flag for Direct Narrowband Filter 4	unitless
	barnard_badflag_filter5	rejection flag for Direct Narrowband Filter 5	unitless
sgp15swfanalsirs1longC1.c1	cloudfraction	Estimated Average Fractional Sky Cover over the Hemispheric Dome (cf)	unitless
sgparsclbnd1clothC1.c1	cloudbasebestestimate	LASER Cloud Base Height Best Estimate	m AGL

11

Appendix B - Output Variables

Table 2 lists the detail description of the variables for the MFRSRCLDOD1MIN VAP output file.

Table 2.   Output Variables

Fieldname	Description	Units
base_time	Base Time in Epoch	seconds since 1970/01/01 00:00:00
time_offset	Time offset from base_time	seconds since base_time
time	Time offset from midnight	seconds since midnight
optical_depth_instaneous	Cloud Optical Depth (Instaneous	unitless
effective_radius_instaneous	Effective Radius (Instaneous)	microns
optical_depth_average	Cloud Optical Depth (Average)	unitless
effective_radius_average	Effective Radius (Average)	microns
cldtaui_error1	Cloud Taui Error1 (1% uncertainty in total irradiance)	unitless
cldtaui_error2	Cloud Taui Error2 (5% uncertainty in Inought)	unitless
cldtaui_error3	Cloud Taui Error3 (uncertainty in liquid water path (LWP) 0.015mm larger)	unitless
cldtaui_error4	Cloud Taui Error4 (20% uncertainty in surface albedo)	unitless
cldtaui_error5	Cloud Taui Error5 (uncertainty in 3um higher of effective radius when there is no MWR data)	unitless
cldtaui_toterror	Instantaneous Cloud Tau Total Uncertainty	unitless
cldtaua_error1	Cloud Taua Error1 (1% uncertainty in total irradiance)	unitless
cldtaua_error2	Cloud Taua Error2 (5% uncertainty in Inought)	unitless
cldtaua_error3	Cloud Taua Error3 (uncertainty in liquid water path (LWP) 0.015mm larger)	unitless
cldtaua_error4	Cloud Taua Error4 (20% uncertainty in surface albedo)	unitless
cldtaua_toterror	Average Cloud Tau Total Uncertainty	unitless
reffi_error1	Effective Radiusi Error1 (1% uncertainty in total irradiance)	microns
reffi_error2	Effective Radiusi Error2 (uncertainty is standard deviation of calibrated 10 Inought points)	microns
reffi_error3	Effective Radiusi Error3 (uncertainty in liquid water path (LWP) 0.001mm larger, using scaling factor with 0.015 mm)	microns
reffi_error4	Effective Radiusi Error4 (uncertainty is 0.01 in surface albedo)	microns
reffi_toterror	Instaneouse Effective Radius Total Error	microns
reffa_error1	Effective Radiusa Error1 (1% uncertainty in total irradiance)	microns
reffa_error2	Effective Radiusa Error2 (uncertainty is standard deviation of calibrated 10 Inought points)	microns
reffa_error3	Effective Radiusa Error3 (uncertainty in liquid water path (LWP) 0.001mm larger, using scaling factor with 0.015 mm)	microns
reffa_error4	Effective Radiusa Error4 (uncertainty is 0.01 in surface albedo)	microns
reffa_toterror	Average Effective Radius Total Error	microns
cosine_solar_zenith_angle	Cosine Solar Zenith Angle	unitless
total_transmittance_filter1	Diffuse Transmission of Narrowband Hemispheric Irradiance, Filter 1	unitless
total_transmittance_filter2	Diffuse Transmission of Narrowband Hemispheric Irradiance, Filter 2	unitless
total_transmittance_filter3	Diffuse Transmission of Narrowband Hemispheric Irradiance, Filter 3	unitless
total_transmittance_filter4	Diffuse Transmission of Narrowband Hemispheric Irradiance, Filter 4	unitless
total_transmittance_filter5	Diffuse Transmission of Narrowband Hemispheric Irradiance, Filter 5	unitless

Table 2. (cont'd)

Fieldname	Description	Units
direct_transmittance_filter1	Direct tranmittance of Narrowband Direct Normal Irradiance, Filter 1	unitless
direct_transmittance_filter2	Direct tranmittance of Narrowband Direct Normal Irradiance, Filter 2	unitless
direct_transmittance_filter3	Direct tranmittance of Narrowband Direct Normal Irradiance, Filter 3	unitless
direct_transmittance_filter4	Direct tranmittance of Narrowband Direct Normal Irradiance, Filter 4	unitless
direct_transmittance_filter5	Direct tranmittance of Narrowband Direct Normal Irradiance, Filter 5	unitless
pwv	Total water vapor along MWR LOS path	cm
lwp	Total liquid water along LOS path, it could come from either MWR or the MFRSR with an assumed effective radius	mm
ir_temp	IR Brightness Temperature	K
cloudfraction	Estimated Average Fractional Sky Cover over the Hemispheric Dome (cf)	unitless
cloudbasebestestimate	Cloud Base Height Best Estimate	m AGL
lwp_uncertainty	LWP uncertainty if derived from MFRSR	mm
lwp_source	LWP Source, =1 from MWR, =2 from MFRSR data, =0 from other	unitless
Io_time	Langley time series	Day fraction offset from 00:00 on this day
Io_filter1	solar constant corrected for solar distance for the Direct Narrowb and Filter1	W/(m^2 nm)
Io_filter2	solar constant corrected for solar distance for the Direct Narrowb and Filter2	W/(m^2 nm)
Io_filter3	solar constant corrected for solar distance for the Direct Narrowb and Filter3	W/(m^2 nm)
Io_filter4	solar constant corrected for solar distance for the Direct Narrowb and Filter4	W/(m^2 nm)
Io_filter5	solar constant corrected for solar distance for the Direct Narrowb and Filter5	W/(m^2 nm)
Io_flag_filter1	Inought flag rejection flag for Direct Narrowband Filter1	unitless
Io_filter1_final	The final Inought that used to determine total transmission	W/(m^2 nm)
cal_start_date	Start day for the Io data selected for calibration	Day fraction offset from 00:00 on this day
cal_end_date	End day for the Io data selected for calibration	Day fraction offset from 00:00 on this day
Io_filter1_standard_deviation	Standard deviation of Inought to the closest 10 points around the run day	W/(m^2 nm)